

PAPER • OPEN ACCESS

## Thermal post-treatment and material characterization of laser powder bed fusion additively manufactured Ti-6Al-4V

To cite this article: Abhinav Anand *et al* 2023 *IOP Conf. Ser.: Mater. Sci. Eng.* **1296** 012016

View the [article online](#) for updates and enhancements.

You may also like

- [Fatigue performance of selective laser melted Ti6Al4V components: state of the art](#)  
Behzad Fotovati, Navid Namdari and Amir Dehghanghadikolaei
- [Heat Treatment Degrading the Corrosion Resistance of Selective Laser Melted Ti-6Al-4V Alloy](#)  
Nianwei Dai, Junxi Zhang, Yang Chen et al.
- [High-pressure coolant effect on the surface integrity of machining titanium alloy Ti-6Al-4V: a review](#)  
Wentao Liu and Zhanqiang Liu

**PRIME**  
PACIFIC RIM MEETING  
ON ELECTROCHEMICAL  
AND SOLID STATE SCIENCE

HONOLULU, HI  
Oct 6-11, 2024

Abstract submission deadline:  
**April 12, 2024**

Learn more and submit!

**Joint Meeting of**  
The Electrochemical Society  
•  
The Electrochemical Society of Japan  
•  
Korea Electrochemical Society

# Thermal post-treatment and material characterization of laser powder bed fusion additively manufactured Ti-6Al-4V

Abhinav Anand<sup>1,2</sup>, Nagarajan Devarajan<sup>2</sup>, Rohit Kumar Gupta<sup>3</sup>, Nikhil Kamboj<sup>1,4</sup>, Ashish Ganvir<sup>1</sup>

<sup>1</sup> Research group of Digital Manufacturing and Surface Engineering, Department of Mechanical and Materials Engineering, University of Turku, FI-20500 Turku, Finland

<sup>2</sup> Department of Metallurgical and Materials Engineering, National Institute of Technology, Tiruchirappalli, Tamil Nadu, 620015, India

<sup>3</sup> Vikram Sarabhai Space Centre, Thiruvananthapuram 695022, India

<sup>4</sup> Department of Biomaterials Science, Faculty of Medicine, Institute of Dentistry, Turku Clinical Biomaterials Centre, University of Turku, 20014, Turku, Finland

E-mail: abhinitt521@gmail.com

**Abstract.** Laser powder bed fusion of Ti-6Al-4V (PBF-LB/Ti-6Al-4V) alloy results in the formation of non-equilibrium microstructures due to very high cooling rates, causing them to be unfit for direct applications; therefore, post-heat-treatment operations are required. This paper investigates the effects of different heat treatment operations on the microstructure, hardness and phase composition of as-built PBF-LB/Ti-6Al-4V samples. Six sets of heat-treatment operations have been designed in which samples have been first subjected to either above or below the beta ( $\beta$ ) transus zone of 980 °C, then subjected to air cooling or water quenching followed by ageing at 510 °C. The novelty of this article is performing double quenching on as-built Ti-6Al-4V parts. Optical microscopy, Vickers microhardness testing, and XRD analysis have been performed on heat-treated samples for material characterization. Microstructural studies have revealed that depending upon the cooling medium and subjected temperature during heat treatment, the extent of dissolution of martensitic ( $\alpha'$ ) needle-like phases present in as-built samples into  $\alpha$ - $\beta$  phase varies, resulting in variation of hardness values. XRD analysis confirmed the presence of  $\beta$ -phase along with the  $\alpha$ -phase in the matrix in air-cooled heat-treated samples. Maximum hardness was obtained in the case when the sample was solutionized at 1050 °C, followed by water quenching and ageing due to the formation of intermetallic precipitates.

**Keywords:** Heat treatment, Ti-6Al-4V, Selective laser melting, Double quenching, Phase transformation

## 1. Introduction

Ti-6Al-4V is one of the most sought-after and widely used titanium alloys in aerospace and biomedical applications due to its high strength-to-weight ratio, good corrosion resistance, and biocompatibility. It is also referred to as alpha( $\alpha$ )+beta( $\beta$ ) titanium alloy because it consists of a combination of both phases



in its microstructure. The  $\alpha$ -phase is a hexagonal close-packed crystal structure stabilized by aluminium (6 weight %), whereas the  $\beta$ -phase is a body-centred cubic crystal structure stabilized by vanadium (4 weight %) [1]. The production of Ti-6Al-4V alloys by conventional manufacturing is challenging due to its high melting temperature, low thermal conductivity, and high chemical reactivity. Moreover, the high cost of manufacturing, longer lead time and suboptimal use of raw materials are major barriers to traditional manufacturing routes. Additive manufacturing (AM) solves these issues and produces parts with complex geometries that are difficult to achieve through conventional routes, along with design freedom for specific end-use applications [2,3]. Laser powder bed fusion (PBF-LB) is the most used AM process for this purpose.

The microstructure of Ti-6Al-4V obtained via casting or forging consists of a mixture of alpha and beta phases, i.e., lamellar, bimodal or equiaxed, which can be later altered by adjusting the thermal history or processing routes, such as thermo-mechanical processing [1]. However, in the case of PBF-LB, due to the very high cooling rate of the melt pool (range of  $10^3$  to  $10^8$  kelvin/second), the obtained microstructure consists of mostly acicular ( $\alpha'$ ) martensitic phase, which results in high-strength but minimal ductility [4]. Also, due to very short interaction time and localized heat inputs, the parts fabricated by PBF-LB have high thermal gradients resulting in thermal stress build-up. The as-printed microstructure consists of non-equilibrium phases accompanied by segregation and is anisotropic due to rapid solidification and complex heating-cooling cycles involved during AM. Therefore, a post-heat treatment operation is required to eliminate residual stress and enhance the mechanical properties of the as-built part by obtaining a microstructure that can yield an optimum combination of ductility and enhanced structural stability [1].

In the case of Ti-6Al-4V, the  $\alpha$ - $\beta$  phase matrix transform entirely into  $\beta$  phase above  $980^\circ\text{C}$ , which is referred to as  $\beta$ -transus temperature [5]. In this study, several post-heat treatment operations, including air cooling and water quenching followed by ageing, have been performed on PBF-LB/Ti-6Al-4V samples to understand the effect of cooling or quenching from above or below the  $\beta$  transus temperature. Also, the effects of double quenching, which has not been reported before, have been investigated in this study.

## 2. Materials and Methods

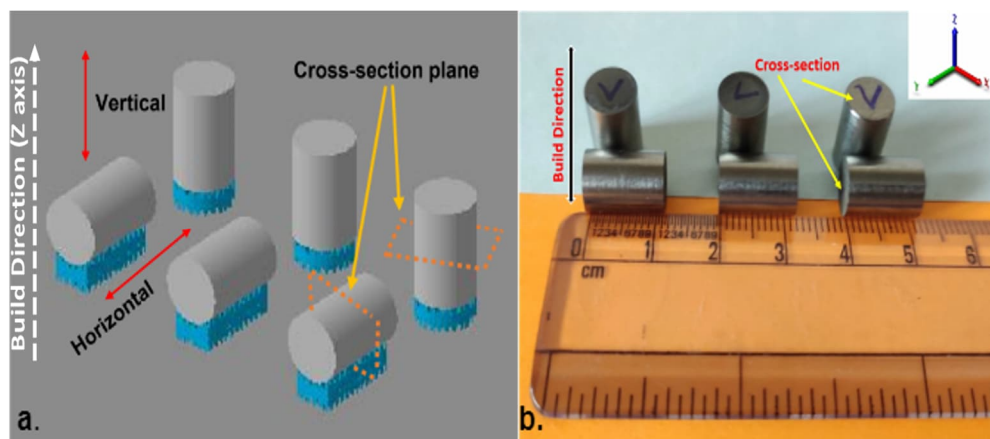


**Figure 1.** a) CAD image showing specimens orientation before printing and highlighting cross-section planes used for study b) PBF-LB/Ti-6Al-4V specimens with build direction along the Z-axis.

Two sets of samples with vertical (V) and horizontal (H) build having a diameter of 8 mm and height of 12 mm were printed using EOS M290 PBF machine as shown in **Figure 1**. The powder size used during the fabrication lied between 20 to  $60\ \mu\text{m}$ . “Chess-board pattern” scanning strategy was used during printing, i.e., 90 degrees rotation of laser beam for every other layer of the print. This strategy was

adopted to improve print quality by evenly distributing the heat across the entire print and minimizing the risk of warping during printing. A laser power of 340 W with a scan speed of 1200 mm/s and a hatch distance of 0.1 to 0.14 mm was used. The powder layer thickness during printing was 60  $\mu\text{m}$ . Each as-built sample was cut into equal halves across the cross-section planes via wire cut EDM to obtain a total of twelve specimens (six horizontal, six vertical) out of three, each H and V, with dimensions of diameter 8 mm and height 6 mm.

Six different heat treatment operations, as shown in **Table 1**, were performed on different sets of samples, each set containing one horizontal and one vertical sample. The heating temperatures were chosen in accordance to study the effect of air-cooling and quenching followed by ageing from the above/below transus temperature of 980 °C. All heat treatments were performed in a box furnace without vacuum manufactured by Nano Tec Pvt. Ltd. with a heating rate of 7 °C/minute.

**Table 1.** Details on the six distinct heat treatments employed for each set of PBF-LB specimens.

Treatment number	Heat treatment details
1 // 2 // 3	Holding for 30 min at 730 °C // 950 °C // 1050 °C, followed by AC to room temperature
4 // 5	Holding for 30 min at 950 °C // 1050 °C, followed by WQ + Ageing at 510 °C for 8 h and then AC to room temperature
6	Holding for 30 min at 1050 °C followed by WQ + Solution treatment at 950 °C for 30 min followed by WQ + Ageing at 510 °C for 8 h and then AC to room temperature

Note: here AC and WQ denote air cooling and water quenching, respectively.

Microscopic analysis was performed after every heat treatment step and also on the as-printed samples. Samples were ground to a fine 2000-grit size using SiC paper and were polished using alumina suspension. Kroll's reagent with a composition of 2 ml H.F., 6 ml HNO<sub>3</sub> and 50 mL distilled water was used to reveal the microstructure of polished samples. Microscopy was performed using Olympus optical microscope with an image analyzer. Microhardness testing was performed on hot-mounted samples using Vickers microhardness testing with an applied load of 1000 gram-force with a ten-second dwell time. Eight indentations were marked during testing, and an average hardness value and mean standard deviation were calculated. Further, XRD was performed on heat-treated samples to identify the type of phase formed using Cu-K $\alpha$  radiation for recording the data in a 2 $\theta$  range of 20° to 90°.

### 3. Results and discussion

#### 3.1. As-built PBF-LB/Ti-6Al-4V

The observed microstructure for the as-built parts is shown in **Figure 2**. The unetched surface was observed under the microscope to reveal the porosities formed during the printing process, possibly due to lack of fusion, partial melting or due to entrapment of gases. As shown earlier in **Figure 1**, the horizontally printed samples are cross-sectioned in such a way that the plane of microstructural examination lies along the build direction, whereas in the case of vertical samples, the cross-section plane is along the laser-scanning direction. The slightly higher average hardness of the horizontal sample ( $356.4 \pm 6.9$  HV) compared to the vertical sample ( $350.6 \pm 7.9$  HV) is due to the faster cooling of the material resulting from the higher thermal flows present in the former build configuration [6].

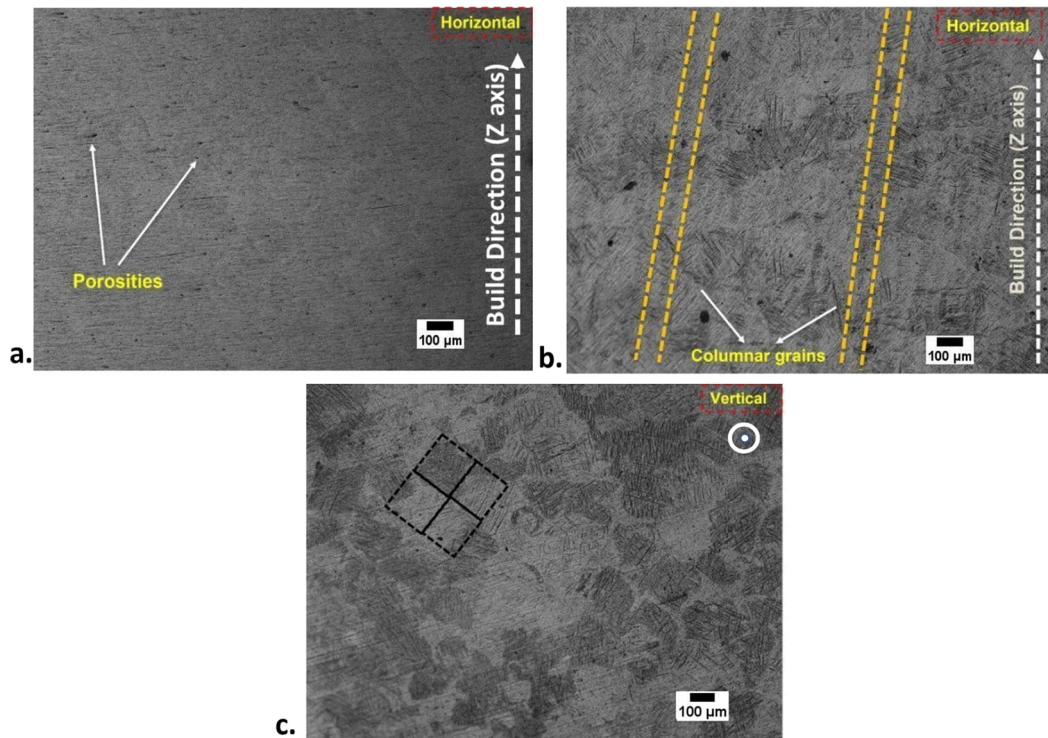


**Figure 2.** a) Polished unetched surface of the as-built part (horizontal) b) Microstructure of horizontal sample revealing columnar grains along the build direction c) Chess-board pattern observed in the cross-sectioned vertical sample (perpendicular to build direction)

Rapid cooling during laser powder bed fusion process resulted in the formation of acicular martensite ( $\alpha'$ ), transforming from the original columnar  $\beta$  grains. The formation of a columnar shape is attributed to the epitaxial growth of the initial  $\beta$  phase caused by successive layer deposition and directional cooling in the build direction, as shown in **Figure 2(b)**. Chess-board patterns, as highlighted in **Figure 2(c)**, have been formed due to the adopted laser scanning strategy used during the printing.

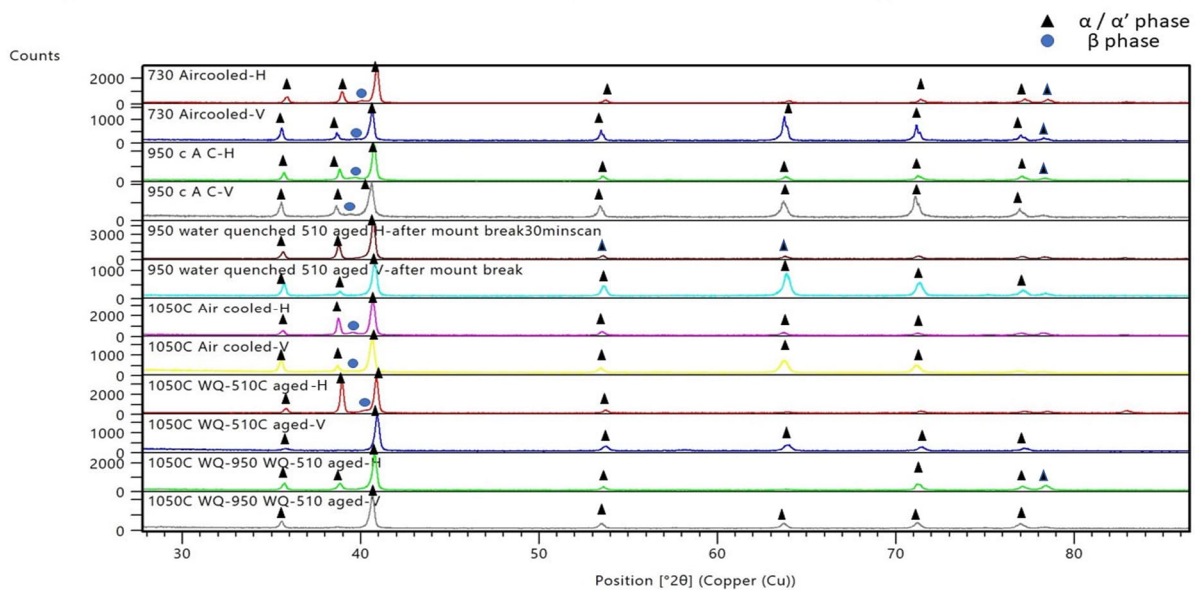


**Figure 3.** The XRD patterns of the heat-treated samples (H-horizontal, V-vertical, AC-air cooled, WQ-water quenched).

### 3.2. Effects of air cooling on PBF-LB/Ti-6Al-4V

X-ray diffraction (XRD) patterns of heat-treated samples have been shown in **Figure 3**. Since both  $\alpha'$  and  $\alpha$  phases have the same hexagonal close-packed crystalline structure, they produce XRD peaks at the same angular position, so they have been indicated as  $\alpha/\alpha'$  in the XRD pattern [7]. The presence of the  $\beta$  phase, as indicated by the XRD study and the shifting of XRD peaks towards the left with an increase in soaking temperature has proved that the air cooling-based heat treatment results in the decomposition of acicular martensitic ( $\alpha'$ ) into  $\alpha+\beta$ , and the transformation of  $\alpha$  into  $\beta$  phase increases with increase in solution temperature. According to previous studies, the equilibrium  $\alpha$ -fractions get reduced to 23 % at 950 °C from around 90 % at 730 °C [8].

As highlighted in **Figure 4**, the microstructural studies indicate the same outcome. Acicular martensitic ( $\alpha'$ ) are no longer visible in samples cooled from 950 °C, and a lamellar  $\alpha+\beta$  phase is formed. Also, the prior  $\beta$  grains begin to disappear during heat treatment and get diffused at 950 °C. When the sample is heated above the  $\beta$ -transus temperature of 980 °C, i.e. at 1050 °C, semi-equiaxed  $\beta$  grains are formed by replacing the columnar  $\beta$  grains, resulting in an  $\alpha$ -Widmanstätten microstructure or basket weave structure. Also, the chess-board pattern in the microstructure of vertical samples begins to disappear by air cooling from 950 °C and vanishes at 1050 °C.

The measured Vickers microhardness of heat-treated samples has been represented in **Figure 5**. The decrease in the hardness of as-built specimens upon air cooling is due to the acicular martensitic ( $\alpha'$ ) phase decomposition. With an increase in solution temperature from 730 °C to 950 °C, a further decrease in values was observed due to the increased  $\beta$  phase in the matrix. But at 1050 °C, an increase in hardness was observed due to formation of Widmanstätten microstructure [9].

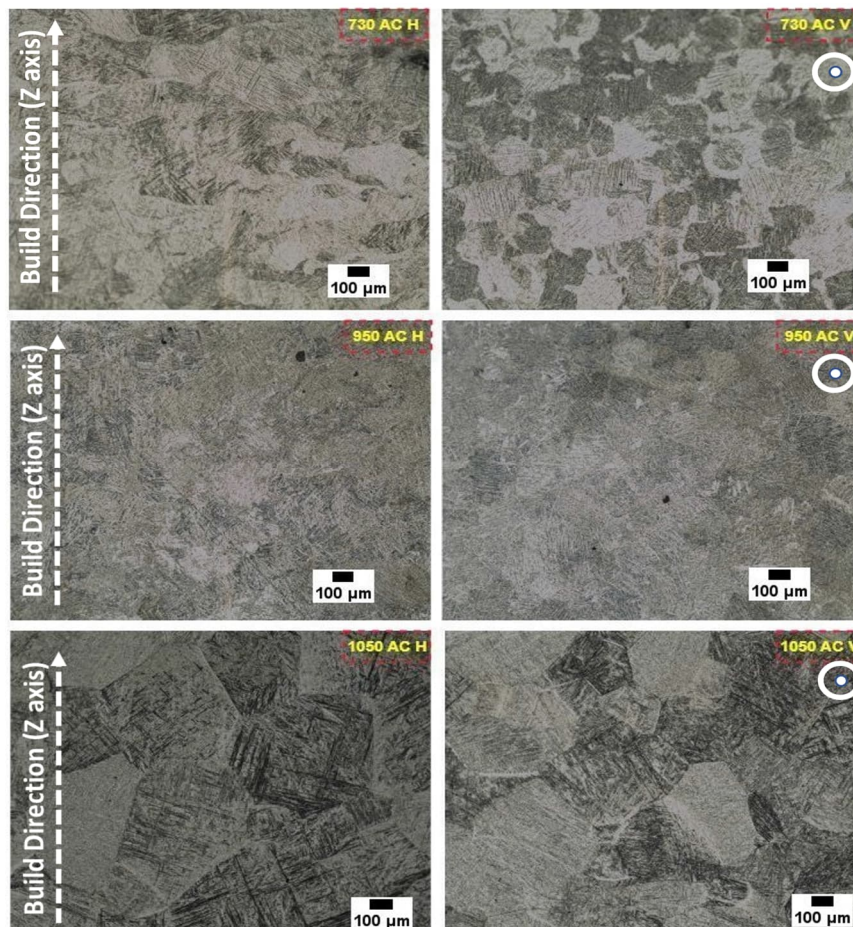


**Figure 4.** The observed microstructures of the samples after being heat-treated for 30 minutes at a) 730 °C, b) 950 °C, c) 1050 °C, followed by air-cooling (AC-air cooling, H-horizontal, V-vertical)

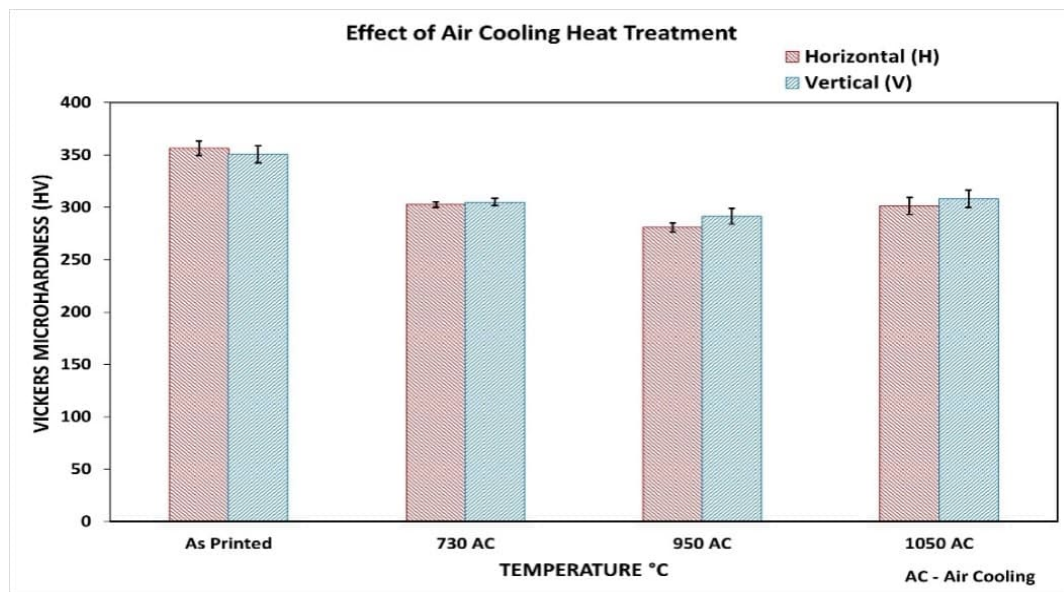


**Figure 5.** Vickers microhardness of heat-treated specimens (air cooled) compared to as-built specimens.

### 3.3. Effects of quenching and ageing on PBF-LB/Ti-6Al-4V

Since the martensite start temperature ( $M_s$ ) for Ti-6Al-4V is  $\sim 900$  °C [10], upon quenching above this temperature, martensitic phases were observed in the matrix. Upon quenching from 950 °C, a microstructure containing lamellar  $\alpha$  phase along with acicular martensite ( $\alpha'$ ) needles were observed, as shown in **Figure 6(a, b)**. Upon subjecting the specimens to a solution temperature below the  $\beta$ -transus temperature, almost all the previous existing acicular martensite ( $\alpha'$ ) (formed during PBF-LB) get decomposed into  $\alpha$  and  $\beta$  phases, and when the quenching is performed from above  $M_s$ , the  $\beta$  phase transform into martensitic phase, leaving behind the primary  $\alpha$  into the matrix. The prior  $\beta$  microstructure containing the laser scan pattern, as shown in **Figure 6(b)**, was retained in this case. The decomposition of martensitic needles was noticed upon ageing the quenched samples for 8 hours. However, the amount of  $\beta$  phase formed after ageing was too low to get detected in the XRD pattern (**Figure 3**).

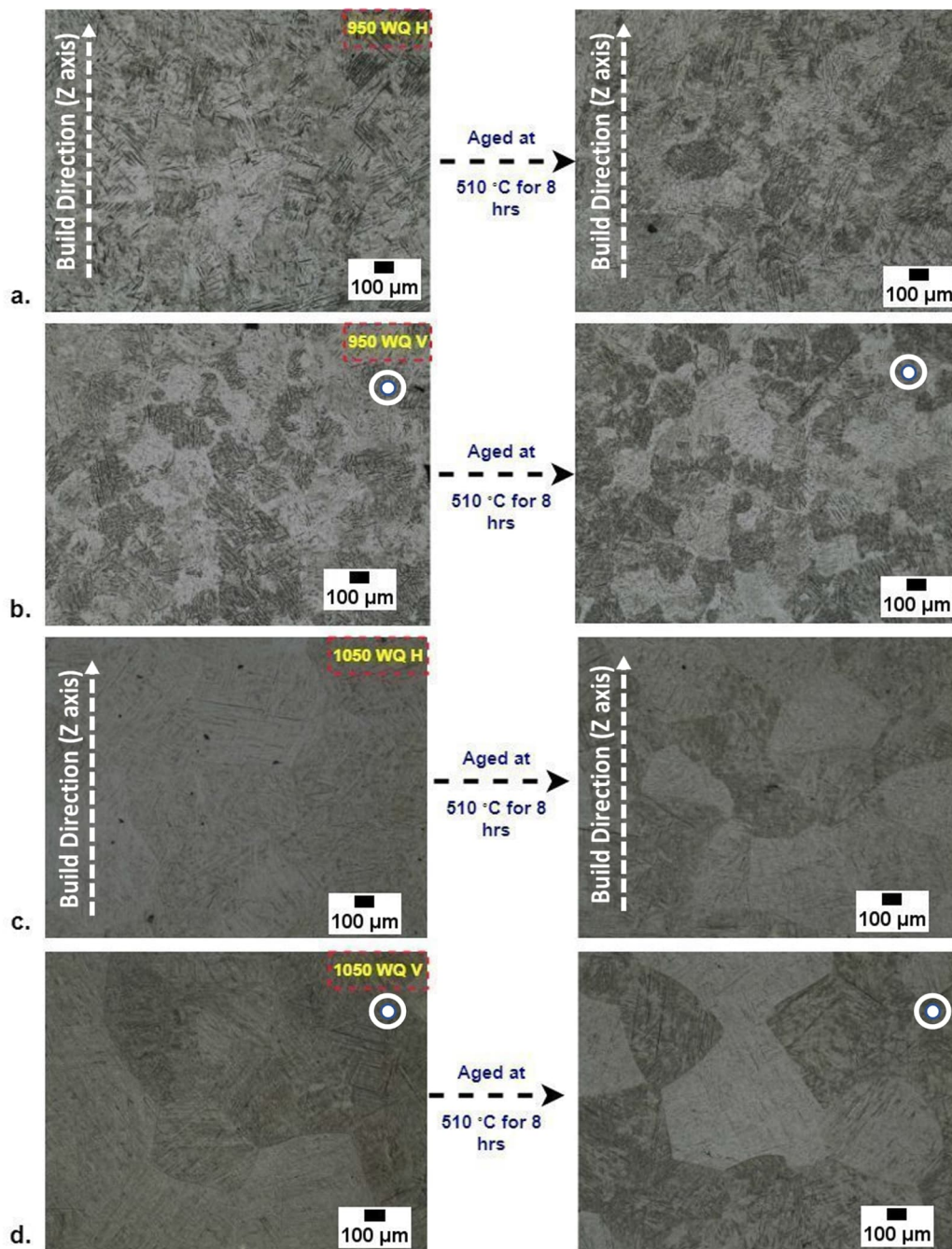


**Figure 6.** Observed microstructures after as-built specimens were subjected to quenching from different temperatures followed by ageing a,b) at 950 °C c,d) at 1050 °C (H-horizontal, V-vertical, WQ-water quenched)

In the case of quenching from above the  $\beta$ -transus temperature, i.e., from 1050 °C, a 100 % martensitic phase originating from the new equiaxed  $\beta$  grains was observed (**Figure 6** (c, d)). Shearing of previously existing columnar grains generated during PBF-LB took place, and the previously existing acicular martensitic phase completely transformed into  $\beta$  phases upon solutionizing at 1050 °C. Upon quenching, this resulted in the formation of weave-type acicular ( $\alpha'$ ) martensite inside equiaxed  $\beta$  grains. Also, the microstructure containing the chess-board laser scan pattern vanished in this case. Furthermore, when the samples were aged, the  $\beta$  phase was detected in the XRD (**Figure 3**), verifying the decomposition of acicular  $\alpha'$  martensite upon ageing above 500 °C.

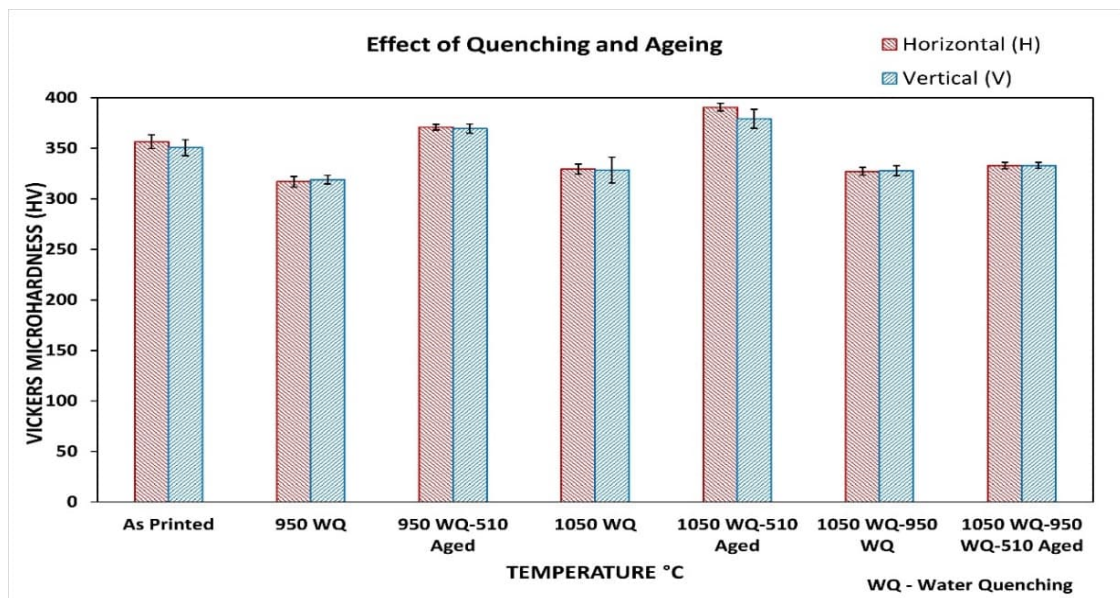


**Figure 7.** Vickers microhardness values calculated after quenching and ageing.

**Figure 7** shows a decrease in hardness value when the samples were quenched from 950 °C and 1050 °C compared to as-built specimens. Since during the water-quenching, the quenching rate is much lower than the quenching due to rapid solidification in PBF-LB, thicker martensitic needles were observed (**Figure 6**) compared to as-built specimens (**Figure 2**). Since the finest microstructure gives more hardness [11], a dip in hardness value is justified. Also, the samples quenched from 1050 °C showcased higher hardness than those quenched from 950 °C because the former has a 100 % martensitic structure, whereas the latter has acicular martensite accompanied by primary  $\alpha$ , which leads to a softer matrix. Moreover, upon ageing, a significant increase in hardness was noticed for both quenching operations. This is possibly contributed by the precipitation of intermetallic Ti-Al phases in the matrix. A previous study has shown that when a quenched Ti-6Al-4V is subjected to ageing between 500 to 900 °C, the intermetallic phases get precipitated in the matrix due to the low solubility of Al in Ti in this temperature range [12].

### 3.4. Effect of double quenching followed by ageing on PBF-LB/Ti-6Al-4V

During double quenching, the samples were first solutionized above  $\beta$ -transus temperature. i.e., at 1050 °C. This resulted in the formation of equiaxed  $\beta$  grains containing weave-type acicular  $\alpha'$  martensite. When the samples were again solutionized at below  $\beta$ -transus temperature. i.e., at 950 °C, most of acicular  $\alpha'$  martensite transformed into  $\alpha+\beta$  phases and upon quenching, the  $\beta$  phases in the matrix transformed again into acicular  $\alpha'$  martensite. However, this time, compared to a normal 950 °C quenching (**Figure 6(a,b)**), the observed microstructure (**Figure 8(a,b)**) has primary  $\alpha$  and martensite originating inside equiaxed  $\beta$  grains, which were formed when the sample was initially heated to 1050 °C. The difference in microstructures resulted in a noticeable change in hardness values of 950 °C WQ and double-quenched samples. Also, the softer primary  $\alpha$  phase contributed to a lower hardness of double-quenched samples compared to as-built and 1050 °C WQ.

However, unlike the ageing of 950 °C WQ and 1050 °C WQ samples, no significant changes in hardness values were observed upon ageing the double-quenched samples (**Figure 7**). Also, no  $\beta$  phase was detected this time in the XRD pattern after ageing. A possible explanation is that double quenching can reduce the amount of precipitates (based on TiAl) that can form in the matrix by disrupting the diffusion of alloying elements and the nucleation of precipitates. Nevertheless, more research needs to be done in this regard to derive a conclusion.

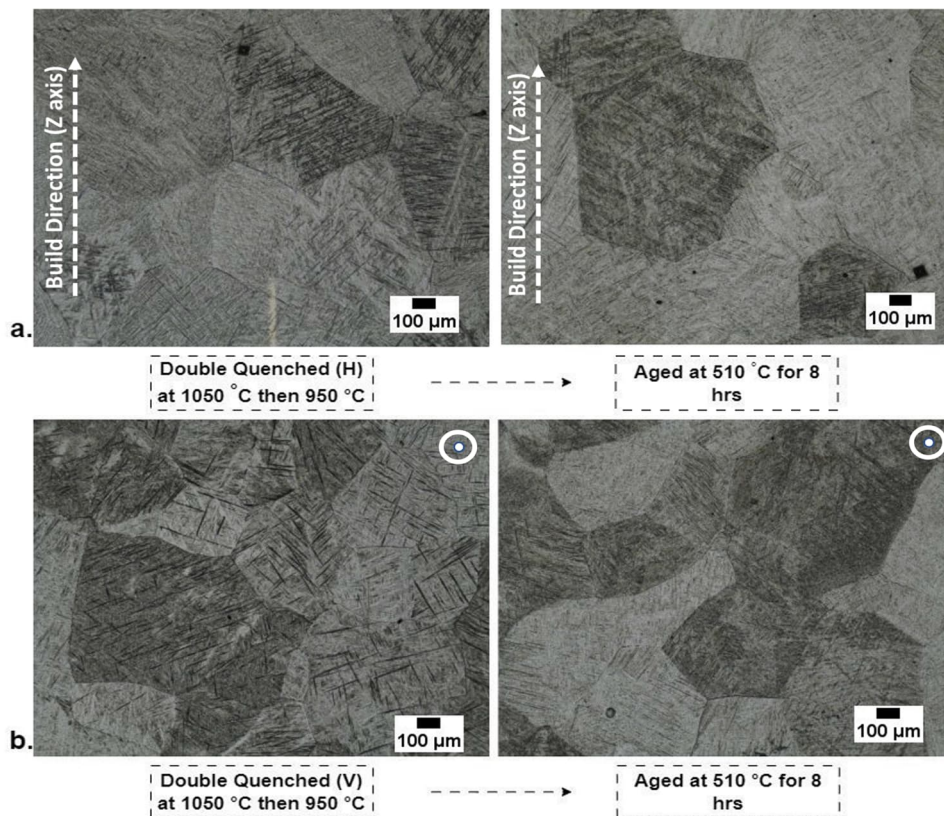


**Figure 8.** Observed microstructures when the as-printed samples get quenched at 1050 °C, followed by quenching again at 950 °C and then aged at 510 °C

#### 4. Conclusions

In this paper, a detailed study was conducted on the heat treatment of as-built PBF-LB/Ti-6Al-4V samples. Optical microscopy, Vickers microhardness test and XRD were performed for material characterization. The following conclusions can be derived from the study:

- As-built horizontal (H) samples constitute prior  $\beta$  columnar grains containing acicular martensitic phase in the matrix, whereas microstructure highlighting chess-board laser scanning pattern was observed in as-built vertical (V) samples.
- Air cooling from 730 °C, 950 °C, and 1050 °C decreases hardness values due to the decomposition of the acicular martensitic phase into  $\alpha$  and  $\beta$  phases.
- Air cooling from above  $\beta$ -transus temperature of 980 °C results in  $\alpha$ -Widmanstätten microstructure, whereas from below  $\beta$ -transus results in lamellar  $\alpha$ + $\beta$  phase.
- Water quenching from above  $\beta$ -transus temperature results in weave-type acicular  $\alpha'$  martensite inside equiaxed  $\beta$  grains, whereas from below beta-transus results in lamellar  $\alpha$  phase along with acicular martensite.
- Water quenching results in a decrease in hardness values as compared to as-built specimens due to an increase in the thickness of the martensite needle due to a slower cooling rate than PBF-LB.
- Upon double quenching, the microstructure contains primary  $\alpha$  and martensitic phases originating inside equiaxed  $\beta$  grains and ageing the double-quenched samples results in no significant change in hardness.

## Acknowledgement-

The authors thank the Group Director of Materials and Metallurgy Group and Deputy Director of Materials and Mechanical Entity for their encouragement and support. They further thank the Director of Vikram Sarabhai Space Centre for permission to publish this work.

## References:

- [1] Polishetty A, Nomani J and Littlefair G 2022 Effect of transus based heat treatment on material characterisation of wrought and additive titanium alloy Ti-6Al-4 V *Mater. Today Proc.* **59** 1749–53
- [2] Lu S L, Zhang Z J, Liu R, Qu Z, Wang B, Zhou X H, Eckert J and Zhang Z F 2022 Prior  $\beta$  grain evolution and phase transformation of selective laser melted Ti6Al4V alloy during heat treatment *J. Alloys Compd.* **914**
- [3] Anand A, Nagarajan D, El Mansori M and Sivarupan T 2022 Integration of Additive Fabrication with High-Pressure Die Casting for Quality Structural Castings of Aluminium Alloys; Optimising Energy Consumption *Trans. Indian Inst. Met.*
- [4] Sun S, Zhang D, Palanisamy S, Liu Q and Dargusch M S 2022 Mechanical properties and deformation mechanisms of martensitic Ti6Al4V alloy processed by laser powder bed fusion and water quenching *Mater. Sci. Eng. A* **839**
- [5] Liu S and Shin Y C 2019 Additive manufacturing of Ti6Al4V alloy: A review *Mater. Des.* **164** 107552
- [6] Palmeri D, Buffa G, Pollara G and Fratini L 2021 The Effect of Building Direction on Microstructure and Microhardness during Selective Laser Melting of Ti6Al4V Titanium Alloy *J. Mater. Eng. Perform.* **30** 8725–34
- [7] Ju J, Zhao C, Kang M, Li J, He L, Wang C, Li J, Fu H and Wang J 2021 Effect of heat treatment on microstructure and tribological behavior of Ti–6Al–4V alloys fabricated by selective laser melting *Tribol. Int.* **159**
- [8] Al-Bermani S S, Blackmore M L, Zhang W and Todd I 2010 The Origin of Microstructural Diversity, Texture, and Mechanical Properties in Electron Beam Melted Ti-6Al-4V *Metall. Mater. Trans. A* **41** 3422–34
- [9] Vrancken B, Thijs L, Kruth J P and Van Humbeeck J 2012 Heat treatment of Ti6Al4V produced by Selective Laser Melting: Microstructure and mechanical properties *J. Alloys Compd.* **541** 177–85
- [10] Wu S Q, Lu Y J, Gan Y L, Huang T T, Zhao C Q, Lin J J, Guo S and Lin J X 2016 Microstructural evolution and microhardness of a selective-laser-melted Ti-6Al-4V alloy after post heat treatments *J. Alloys Compd.* **672** 643–52
- [11] Vilaro T, Colin C and Bartout J D 2011 As-fabricated and heat-treated microstructures of the Ti-6Al-4V alloy processed by selective laser melting *Metall. Mater. Trans. A Phys. Metall. Mater. Sci.* **42** 3190–9
- [12] Liang Z, Sun Z, Zhang W, Wu S and Chang H 2019 The effect of heat treatment on microstructure evolution and tensile properties of selective laser melted Ti6Al4V alloy *J. Alloys Compd.* **782** 1041–8